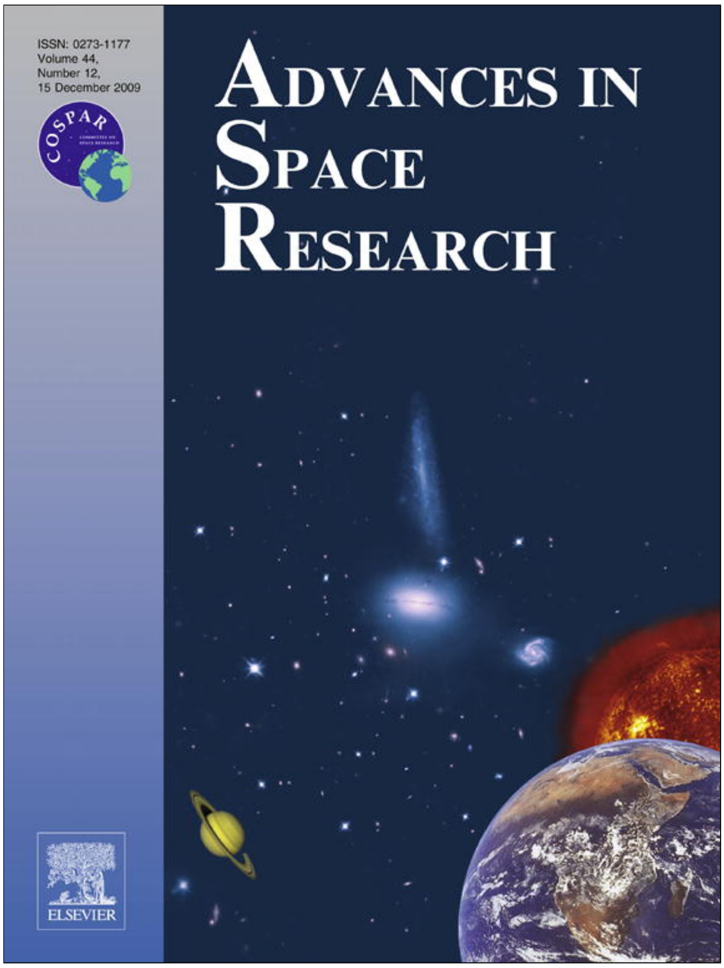
ISSN: 0273-1177
Volume 44,
Number 12,
15 December 2009
COSPAR
ADVANCES IN SPACE RESEARCH
ELSEVIER

Available online at www.sciencedirect.com

ScienceDirect

Advances in Space Research 44 (2009) 1428–1432

ELSEVIER

ADVANCES IN SPACE RESEARCH
(a COSPAR publication)

www.elsevier.com/locate/asr

Using high-energy proton fluence to improve risk prediction for consequences of solar particle events

Myung-Hee Y. Kim [a,*], Matthew J. Hayat [a,1], Alan H. Feiveson [b], Francis A. Cucinotta [b]

[a] Universities Space Research Association, Division of Space Life Sciences, 2101 NASA Parkway, SK/SRPE/B37, Houston, TX 77058, USA
[b] NASA Johnson Space Center, 2101 NASA Parkway, SK/B37, Houston, TX 77058, USA

Received 17 November 2008; received in revised form 26 June 2009; accepted 31 July 2009

Abstract

The potential for exposure to large solar particle events (SPEs) with high energy levels is a major concern during interplanetary transfer and extra-vehicular activities (EVAs) on the lunar and Mars surface. Previously, we have used data from the last 5 solar cycles to estimate percentiles of dose to a typical blood-forming organ (BFO) for a hypothetical astronaut in a nominally shielded spacecraft during a 120-d lunar mission. As part of this process, we made use of complete energy spectra for 34 large historical SPEs to calculate what the BFO mGy-Eq dose would have been in the above lunar scenario for each SPE. From these calculated doses, we then developed a prediction model for BFO dose based solely on an assumed value of integrated fluence above 30 MeV (Φ_{30}) for an otherwise unspecified future SPE. In this study, we reasoned that since BFO dose is determined more by protons with higher energies than by those with lower energies, more accurate BFO dose prediction models could be developed using integrated fluence above 60 (Φ_{60}) and above 100 MeV (Φ_{100}) as predictors instead of Φ_{30}. However to calculate the unconditional probability of a BFO dose exceeding a pre-specified limit ("BFO dose risk"), one must also take into account the distribution of the predictor (Φ_{30}, Φ_{60}, or Φ_{100}), as estimated from historical SPEs. But Φ_{60} and Φ_{100} have more variability, and less available historical information on which to estimate their distributions over many SPE occurrences, than does Φ_{30}. Therefore, when estimating BFO dose risk there is a tradeoff between increased BFO dose prediction at a given energy threshold and decreased accuracy of models for describing the distribution of that threshold over future SPEs as the threshold increases. Even when taking the second of these two factors into account, we still arrived at the conclusion that overall prediction improves as the energy level threshold increases from 30 to 60 to 100 MeV. These results can be applied to the development of approaches to improve radiation protection of astronauts and the optimization of mission planning for future space missions.

Keywords: Space radiation risk; BFO dose risk; Risk assessment; Solar particle events; Radiation protection

1. Introduction

The development of operational strategies and structural capability for the protection of astronauts from solar particle events (SPEs) is an important consideration for the planning of future lunar surface scenarios and a mission to Mars. A major concern for astronauts' safety during space missions is possible acute radiation syndrome from exposure to an intense SPE during an extra-vehicular activity (EVA) or in a lightly shielded vehicle ($<5\,\mathrm{g\,cm^{-2}}$). In addition, multiple exposures to SPEs with intense particle flux and high energy levels are thought to increase the risk of radiation-caused cancer and degenerative disease (Cucinotta, 1999; Cucinotta et al. 2001; Cucinotta and Durante 2006). Most SPEs would produce small crew doses; however even a small SPE can disrupt mission operations and lead to excessive costs. A concern for health risk to astronauts would arise only from a small portion of SPEs (about 10%) where effective doses would be expected to exceed 50 mSv.

* Corresponding author. Tel.: +1 281 244 2993; fax: +1 281 483 3058. *E-mail address:* myung-hee.y.kim@nasa.gov (M.-H.Y. Kim).
[1] Present address: Currently at Johns Hopkins University, 525 N. Wolfe St., Baltimore, MD 21205, USA.

0273-1177/$36.00 © 2009 COSPAR. Published by Elsevier Ltd. All rights reserved.
doi:10.1016/j.asr.2009.07.028

In Kim et al. (2009), for each of the 34 largest historical SPEs, we used spectral data to construct Weibull models for approximating Φ_E, the event-integrated fluence above an arbitrary level of E MeV. Depending on context, we will sometimes use the notation $\Phi(E) \equiv \Phi_E$ to emphasize that Φ_E is a function of E. For the ith SPE, the approximating function was of the form

$$\hat{\Phi}_i(E) = P_i\, exp(-a_i E^{b_i}), \tag{1}$$

where P_i, a_i and b_i are SPE-specific parameters. For each of these 34 SPEs, $\hat{\Phi}_i(E)$ was then used in a physical/physiological model (Billings and Yucker, 1973; Cucinotta et al. 1994; Wilson et al. 1989) to calculate B_i, the mGy-Eq dose to a blood-forming organ (BFO) for a hypothetical astronaut in a nominally shielded spacecraft or lunar habitat. We then developed a log-linear regression model to predict B_i (which was calculated using the entire function $\hat{\Phi}_i(E)$), by a simple function of $\Phi_{30,i}$ alone, where $\Phi_{30,i}$ is the actual observed value of Φ_{30} for the ith SPE. The model was of the form

$$\log B_i = \beta_0 + \beta_1 \log \Phi_{30,i} + u_i, \tag{2}$$

where u_i is a normally distributed random error term with zero mean and variance σ^2.

At the same time, we also used the complete database of 370 SPEs (Feynman et al. 1990; Goswami et al. 1988; King, 1974; NGDC/GOES, 2008; Shea and Smart, 1990) recorded during cycles 19–23 to model (1) the probability distribution of SPE occurrence times for lunar stays of several duration lengths, centered at the times of peak SPE occurrence within a solar cycle; and (2) the probability distribution of Φ_{30} over a range of SPEs that could occur. Finally, we combined the distributions of SPE occurrence times and Φ_{30} with the model given by Eq. (2) to estimate percentiles of BFO dose attributable to future SPEs during hypothetical stays on the moon centered at the time of maximum SPE occurrence. The advantage of this method is that only the probability distribution of Φ_{30} for future SPEs is needed to make this calculation, not the complex distribution of entire energy spectra.

As described in Kim et al. (2009) the absorbed dose $D(x)$ due to energy deposition at given location x by all particles is an integral of the form

$$D(x) = \int_0^\infty \psi(E) dE, \tag{3}$$

where the scaled flux $\psi(E)$ depends on the stopping power of the material at x and on $\varphi_j(x, E)$, the flux of ions of type j with atomic mass A_j having energy E at x ($j = 1, 2, \ldots$). For the scenarios over which we have calculated BFO dose, which depends on $D(x)$, $\psi(E)$ is high, at lower energies ($E < 30$ MeV) corresponding to low proton penetration depth, and $\psi(E)$ falls off most rapidly for larger values of E, where much higher penetration depth occurs. For this reason, we hypothesized that a linear model predicting BFO dose (or for other deep-seated tissues) in terms of $\Phi(60)$ or $\Phi(100)$ would give a better approximation than would Eq. (2). As an example, in Kim et al. (2009), the BFO dose of 180 mGy-Eq calculated from the entire energy spectrum of the SPE with the largest recorded value of Φ_{30} in the space era (9.0×10^9 protons cm^{-2}) was lower than the NASA 30-day BFO dose limit of 250 mGy-Eq (NCRP, 2000; NRC/NAS, 2008). However, BFO doses of 400, 470, and 480 mGy-Eq calculated from the spectra of three other events with smaller Φ_{30} (1.00×10^9, 4.23×10^9, and 5.0×10^9 protons cm^{-2}, respectively), were over the limit. The reason is that the spectra of the latter three events, although they had lower total integrated fluence above 30 MeV, actually had more integrated fluence at higher energy levels than did the first event. In particular, $\Phi_{100} = 3.5 \times 10^8$, 4.58×10^8, and 5.5×10^8 protons cm^{-2}, respectively, for these events as compared with $\Phi_{100} = 2.4 \times 10^8$ for the first event.

However, a mitigating factor when evaluating the expected BFO dose for a lunar mission comprising several SPEs, using a model analogous to Eq. (2) for $E > 30$, is that a good estimate of the probability distribution of Φ_E over SPEs is needed. The detection thresholds especially at high proton energies, differed between the 19th and more recent cycles, therefore an unbiased representation of the distribution of Φ_{60} and Φ_{100} is best obtained using only fluence data from 169 SPEs recorded from 1986 to the present (solar cycles 22 and 23), which are the measurements of the 5-min average integral proton flux for SPEs by Geostationary Operational Environmental Satellite (GOES) spacecraft obtained through direct access to the National Oceanographic and Atmospheric Agency's (NOAA's) National Geophysical Data Center (NGDC). By contrast, in Kim et al. (2009), we were able to use 368 SPEs' fluence from 370 recorded SPEs over cycles 19–23 to estimate the distribution of Φ_{30}. Here, we investigate the tradeoff between BFO dose prediction accuracy and integrated fluence probability distribution estimation accuracy to show that with current data, the best prediction of the total BFO dose over a mission can be made using Φ_{100}, as opposed to using Φ_{60} or Φ_{30}.

2. Predicting BFO dose from integrated fluence over higher proton energies

In the previous work (Kim et al. 2009), calculated BFO mGy-Eq doses (B_i) from 34 historically large SPEs were modeled in terms of Φ_{30} in Eq. (2). Since then, values of B_i have been calculated from the full energy spectra of nine additional SPEs. For these 43 SPEs in total, the model fit greatly improves when predicting B_i using Φ_{60} or Φ_{100}. This can be seen in Fig. 1, which shows scatter plots of $\log_{10} B_i$ vs. $\log_{10} \Phi_{E,i}$ for $E = 30$, 60, and 100 MeV. Estimated values of β_0, β_1, residual error standard deviation, and R^2 for all three log-linear models are summarized in Table 1.

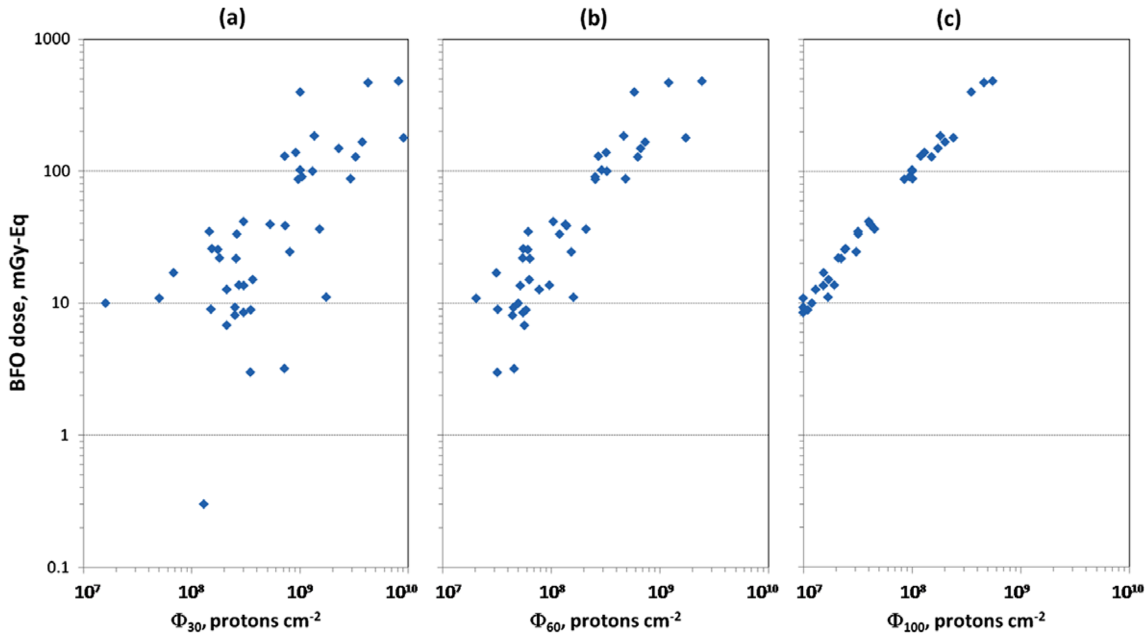

Fig. 1. Predicting BFO mGy-Eq from integrated fluence of (a) Φ_{30}, (b) Φ_{60}, and (c) Φ_{100}.

Table 1
BFO regression models ($N = 43$).

Model	E (MeV)	β_{1E}	β_{0E}	σ_E	R^2
1	30	0.770	−5.214	0.481	0.471
2	60	1.084	−7.304	0.263	0.842
3	100	1.040	−6.336	0.062	0.991

3. Estimation of BFO dose risk for a future SPE during a lunar mission

If the objective of this study were only to predict the BFO mGy-Eq dose based solely on knowledge of Φ_E, clearly the model based on Φ_{100} would be the best choice. However to use this method to calculate the BFO dose risk for future lunar missions, we have to take into account the probability distribution of Φ_E for hypothetical future SPEs. Let Z ($\log_{10}$ mGy-Eq) be the log BFO dose. From the generalization of Eq. (2) for a general value of E and given $\log_{10} \Phi_E = X$, the analogous model for Z is

$$Z = \beta_{0E} + \beta_{1E}X + u_E, \tag{4}$$

where the coefficients β_{0E} and β_{1E} and the variance of the error term u_E depend on E. This model represents how much we know about Z, and by extension the BFO dose, which depends on the full energy spectrum of an SPE through Eq. (3), given the partial information X about the energy spectrum. The error term u_E, which is actually the discrepancy between the true log BFO dose and the approximation $\beta_{0E} + \beta_{1E}X$, reflects random variation of the rest of the energy spectrum of an SPE given that $\log_{10} \Phi_E = X$. As an approximation, we assume $u_E \sim N(0, \sigma_E^2)$. From Table 1, we have already seen that as E increases σ_E decreases, reflecting increased accuracy of the linear approximation.

Let B_0 be a pre-defined critical level of BFO dose, e.g. $B_0 = 250$ mGy-Eq of the NASA 30-day limit (NCRP, 2000; NRC/NAS, 2008) and let $Z_0 = \log_{10} B_0$. Then,

$$\mathrm{P}(\text{BFO dose} > B_0) = \mathrm{P}(Z > Z_0) = P\left(X > \frac{z_0 - \beta_{0E} - u_E}{\beta_{1E}}\right). \tag{5}$$

In Kim et al. (2009), we predicted BFO dose risk by use of Eq. (5) for $E = 30$ MeV with X assumed to follow a Gamma distribution independent of u_E. We now consider the possible use of Φ_{60} or Φ_{100} instead of Φ_{30} for predicting this risk, where for fixed E, X is assumed to have a Gamma distribution with shape parameter λ_E and scale parameter θ_E. More specifically, we will use the notation $X \sim G(\lambda_E, \theta_E)$, meaning that for any $c > 0$,

$$Q_X(c) = P(X > c) = \frac{1}{\theta_E^{\lambda_E}\Gamma(\lambda_E)} \int_c^\infty u^{\lambda_E - 1} e^{-u/\theta_E} du. \tag{6}$$

Combining Eqs. (5) and (6), and using $u_E \sim N(0, \sigma_E^2)$, gives

$$\mathrm{P}(\text{BFO dose} > B_0) = \int_{-\infty}^{\infty} Q_X\left(\frac{z_0 - \beta_{0E} - u}{\beta_{1E}}\right) \phi\left(\frac{u}{\sigma}\right) \frac{1}{\sigma} du, \tag{7}$$

where $\phi(\cdot)$ is the standard normal probability density function. In practice, β_{0E}, β_{1E}, and σ_E are unknown and must be estimated by linear regression of $\log_{10} B_i$ on $\log_{10} \Phi_{E,i}$ for $E = 60$ and 100 MeV as was done in Kim et al. (2009) for $E = 30$ MeV. To compare the models for $E = 60$ or 100 MeV with the one for $E = 30$ MeV, we ran a Monte Carlo study, simulating the estimation of β_{0E}, β_{1E}, and σ_E as well as the Gamma parameters λ_E and θ_E, then

Table 2
Gamma distribution parameters.

Model	E (MeV)	N	λ_E	θ_E	KS
1	30	368	36.5	0.187	0.310
2	60	169	20.9	0.276	0.295
3	100	169	19.3	0.275	0.392

substituted these estimates into Eq. (7). The process was repeated 10,000 times giving rise to empirical distributions of estimates of $P(\text{BFO dose} > B_0)$ for each value of E.

4. Results

4.1. Gamma distribution models

Estimated values of λ_E and θ_E, are shown in Table 2 for $E = 30$, 60, and 100 MeV. As described above, only 169 SPEs (from solar cycles 22 and 23) were used for estimating the distributions of X for $E = 60$ or 100 MeV, as opposed to the 368 SPEs used for the case $E = 30$ MeV. The last column of Table 2 shows the P-value for the Kolmogorv–Smirnov test of the null hypothesis that X has the particular Gamma distribution shown. In all three cases ($P > 0.25$), it can be seen that there was no evidence suggesting significant model misspecification, even with the fairly large sample sizes involved.

4.2. Simulated estimation of BFO dose risk

Results of the Monte Carlo simulation of BFO dose risk in a spacecraft (5 g cm^{-2}) during interplanetary transfer are shown in Fig. 2 for $B_0 = 100(25)300$ mGy-Eq. This figure shows the median estimate as well as the 5th and 95th percentiles of the estimate of $P(\text{BFO dose} > B_0)$, taking account random errors in estimating β_{0E}, β_{1E}, and σ_E with data from 43 SPEs, as well as errors in estimating λ_E and θ_E, from either 368 or 169 SPEs, depending on E. From this figure, it is clear that the much larger value of σ_{30}, leading to larger errors in estimating $\beta_{0,30}$ and $\beta_{1,30}$, makes estimation using Φ_{30} less reliable than using Φ_{60} or Φ_{100}, even though there is more error in estimating the Gamma distributions for the latter two cases based on 169 instead of 368 SPEs. However, there does not appear to be any significant bias caused by using Φ_{30}, as the medians of all three methods agree well over the range of B_0 shown.

5. Summary and conclusions

Astronauts' organ doses due to the exposure to extreme SPEs have been calculated for human exploration missions by many authors (Ballarini et al. 2004; Bernabeu and Casanova 2007; Hoff et al. 2004; Kim et al. 1999; Simonsen et al. 1992; Townsend and Zapp, 1999; Wilson et al. 1991, 1999). Although the potential exposure to large SPEs is a major concern during EVAs on the surface missions and during the interplanetary transit, an accurate assessment of the probability of such occurrences must be informed for the planning and decision of specific scenarios.

In Kim et al. (2009), a probabilistic approach incorporating three stages of modeling was developed using the recorded SPE database of proton fluence measurements

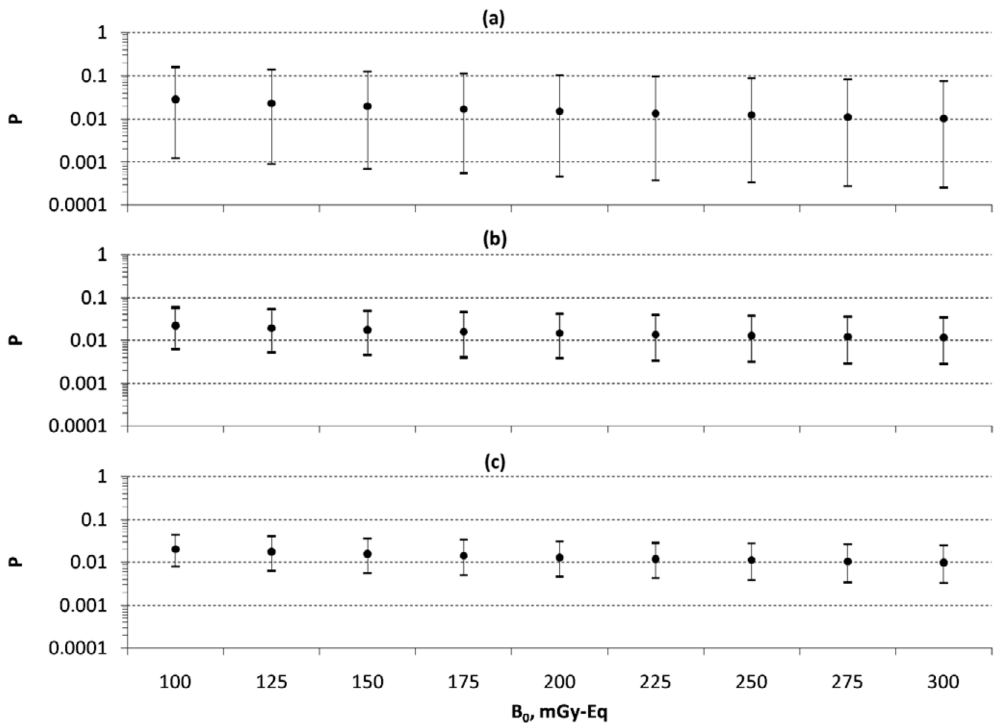

Fig. 2. Estimating probability of BFO dose exceeding pre-defined critical levels of BFO dose, B_0, ranging from 100 to 300 mGy-Eq with 25 mGy-Eq increments using (a) Φ_{30}, (b) Φ_{60}, and (c) Φ_{100}. Centered symbol (●) is for median estimate and lower (⊥) and upper (⊤) limits are for the 5th and 95th percentiles of estimates, respectively.

with energy >30 MeV that have occurred during the past 5 solar cycles. First, the expected number of SPEs for a given mission period was estimated from a non-homogeneous Poisson process model, for which a non-constant hazard function has been defined to represent the propensity of SPE data in space era. Second, the distribution of proton fluence for each event occurrence was simulated with a random draw from a Gamma distribution representing energy above 30 MeV (Φ_{30}). Finally, simulated exposure levels at a typical BFO site inside a spacecraft for one SPE were calculated from a log-linear regression model based on Φ_{30} and combined with the Poisson and Gamma models to simulate the distribution of cumulative dose for lunar missions of various lengths.

Here, it has been shown that the BFO dose for one SPE is much more precisely predicted by proton fluence at high energy, Φ_{100}, than at lower energies, Φ_{30} or Φ_{60}. Despite increased uncertainty with respect estimating the distribution of the proton fluence at higher energies, the overall prediction of BFO dose for a future unspecified SPE was found to be more reliable when basing that prediction on Φ_{100} or on Φ_{60} than on Φ_{30}, with Φ_{100} being the best predictor. We expect this result holds for organ doses for other deep-seated tissues such as lung or stomach, however for the less shielded skin and lens further study should be made.

Because it is not feasible to model the probability distribution of complete energy spectra $\Phi(E)$ $(0 < E < \infty)$ for future SPEs, a practical alternative to accurate assessment of radiation risk from SPEs is to approximate this risk based on the measurements at high energies of protons beyond 100 MeV, which by far have the most weight in the calculation of doses for deep-seated organs. More accurate prediction of BFO dose risk will be useful in developing guidelines to manage space radiation risk for astronauts during future space exploration missions. For example, the projected cost of adding a very small region with more shielding inside a spacecraft (currently considered as 5 g cm^{-2} aluminum) would be justified if it could be shown that this would almost certainly lower the probability of exceeding the NASA 30-d limit of BFO dose to acceptable risk levels for specific lunar mission scenarios. By using Φ_{100} to calculate this probability instead of Φ_{30}, we could be much more sure that the added shielding would indeed be effective in meeting operational risk specifications.

Acknowledgments

This work was supported in part by the NASA Space Radiation Risk Assessment Project and the Living with Star Program's Earth-Moon-Mars Radiation Exposure Module (EMMREM) support at NASA Johnson Space Center.

References

Ballarini, F., Biaggi, M., De Biaggi, L., Ferrari, A., Ottolenghi, A., Panzarasa, A., Paretzke, H.G., Pelliccioni, M., Sala, P., Scannicchio, D., Zankl, M. Role of shielding in modulating the effects of solar particle events: Monte Carlo calculation of absorbed dose and DNA complex lesions in different organs. Adv. Space Res. 34, 1338–1346, 2004.

Bernabeu, J., Casanova, I. Geant4-based radiation hazard assessment for human exploration missions. Adv. Space Res. 40, 1368–1380, 2007.

Billings, M.P., Yucker, W.R. The computerized anatomical man (CAM) model. NASA CR-134043, Washington, DC, 1973.

Cucinotta, F.A. Issues in risk assessment from solar particle events. Radiat. Meas. 30, 261–268, 1999.

Cucinotta, F.A., Durante, M. Cancer risk from exposure to galactic cosmic rays: implications for space exploration by human beings. Lancet Oncol. 7, 431–435, 2006.

Cucinotta, F.A., Wilson, J.W., Badavi, F.F. Extension to the BRYNTRN code to monoenergetic light ion beams. NASA Report No. TP-3472, Washington, DC, 1994.

Cucinotta, F.A., Schimmerling, W., Wilson, J.W., Peterson, L.E., Saganti, P., Badhwar, G.D., Dicello, J.F. Space radiation cancer risks and uncertainties for Mars missions. Radiat. Res. 156, 682–688, 2001.

Feynman, J., Armstrong, T., Dao-Gibner, L., Silverman, S.J. J. Spacecraft 27 (4), 403–410, 1990.

Goswami, J.N., McGuire, R.E., Reedy, R.C., Lal, D., Jha, R. Solar flare protons and alpha particles during the last three solar cycles. J. Geophys. Res. 93 (A7), 7195–7205, 1988.

Hoff, J.L., Townsend, L.W., Zapp, E.N. Interplanetary crew doses and dose equivalents: variations among different bone marrow and skin sites. Adv. Space Res. 34, 1347–1352, 2004.

Kim, M.Y., Wilson, J.W., Cucinotta, F.A., Simonsen, L.C., Atwell, W., Badavi, F.F., Miller, J. Contribution of high charge and energy (HZE) ions during solar-particle event of September 29, 1989, NASA TP-209320, 1999.

Kim, M.Y., Hayat, M.J., Feiveson, A.H., Cucinotta, F.A. Prediction of frequency and exposure level of solar particle events. Health Phys. 97 (1), 68–81, 2009.

King, J.H. Solar proton fluences for 1977–1983 space missions. J. Spacecraft 11 (6), 401–408, 1974.

National Council on Radiation Protection and Measurements (NCRP). Radiation protection guidance for activities in low-Earth orbit. National Council on Radiation Protection and Measurements, Bethesda, Maryland, NCRP Report No. 132, 2000.

National Geophysical Data Center (NGDC). GOES Space Environment Monitor. Available from: <http://goes.ngdc.noaa.gov/data/>. Accessed 4 November 2008.

National Research Council/National Academy of Sciences (NRC/NAS), Committee on the Evaluation of Radiation Shielding for Space Exploration. Managing Space Radiation Risk in the New Era of Space Exploration. The National Academies Press, 2008.

Shea, M.A., Smart, D.F. A summary of major proton events. Solar Phys. 127, 297–320, 1990.

Simonsen, L.C., Atwell, W., Nealy, J.E., Cucinotta, F.A. Radiation dose to critical body organs for October 1989 proton event, NASA TP-3237, 1992.

Townsend, L.W., Zapp, E.N. Dose uncertainties for large solar particle events: input spectra variability and human geometry approximations. Radiat. Meas. 30, 337–343, 1999.

Wilson, J.W., Townsend, L.W., Nealy, J.E., Chun, S.Y., Hong, B.S., Buck, W.W., Lamkin, S.L., Ganapole, B.D., Kahn, F., Cucinotta, F.A. BRYNTRN: a Baryon transport model. NASA Report No. TP-2887, Washington, DC, 1989.

Wilson, J.W., Townsend, L.W., Schimmerling, W., Khandelwal, G.S., Khan, F., Nealy, J.E., Cucinotta, F.A., Simonsen, L.C., Shinn, J.L., Norbury, J.W. Transport methods and interactions for space radiations. NASA Report No. RP 1257, Washington, DC, 1991.

Wilson, J.W., Cucinotta, F.A., Shinn, J.L., Simonsen, L.C., Dubey, R.R., Jordan, W.R., Jones, T.D., Chang, C.K., Kim, M.Y. Shielding from solar particle event exposures in deep space. Radiat. Meas. 30, 361–382, 1999.